

Weak lensing and dark energy

Dragan Huterer

Department of Physics, Enrico Fermi Institute, The University of Chicago, Chicago, Illinois 60637-1433

(Received 26 June 2001; published 12 February 2002)

We study the power of upcoming weak lensing surveys to probe dark energy. Dark energy modifies the distance-redshift relation as well as the matter power spectrum, both of which affect the weak lensing convergence power spectrum. Some dark-energy models predict additional clustering on very large scales, but this probably cannot be detected by weak lensing alone due to cosmic variance. With reasonable prior information on other cosmological parameters, we find that a survey covering 1000 sq deg down to a limiting magnitude of $R=27$ can impose constraints comparable to those expected from upcoming type Ia supernova and number-count surveys. This result, however, is contingent on the control of both observational and theoretical systematics. Concentrating on the latter, we find that the *nonlinear* power spectrum of matter perturbations and the redshift distribution of source galaxies both need to be determined accurately in order for weak lensing to achieve its full potential. Finally, we discuss the sensitivity of the three-point statistics to dark energy.

DOI: 10.1103/PhysRevD.65.063001

PACS number(s): 98.62.Sb, 95.35.+d, 98.80.Es

I. INTRODUCTION

Recent direct evidence for acceleration of the universe [1,2] has spurred considerable activity in finding ways to probe the source of this acceleration, dark energy [3–6] (for a review of dark energy see Ref. [7]). Because dark energy varies with redshift more slowly than matter, it starts contributing significantly to the expansion of the universe only relatively recently, at $z \lesssim 2$. This component is believed to be smooth (or nearly so), and therefore detectable mainly through its effect on the expansion rate of the universe. For these reasons, it is generally believed that type Ia supernovae (SNe Ia) and number-count surveys of galaxies and galaxy clusters have the most leverage to probe dark energy, as they probe the distance and volume in the desired redshift range [8]. Indeed, planned supernova surveys (e.g., SNAP¹) and number-count methods [9,10] are expected to impose tight constraints on the smooth component, for example, $\sigma(w) \approx 0.05$ from SNAP, assuming a flat universe.

The program of weak gravitational lensing (WL) is primarily oriented toward mapping the distribution of matter in the universe. The paths of photons emitted by distant objects and traveling toward us are perturbed due to the intervening mass. The weak lensing regime corresponds to the intervening surface density of matter being much smaller than some critical value; in that case the observed objects (e.g. galaxies) are slightly distorted. The weak lensing distortions are small (roughly at the 1% level) and one needs a large sample of foreground galaxies in order to separate the lensing effect from the “noise” represented by random orientations of galaxies. Therefore, observations of lensed galaxies provides information on the matter distribution in the universe, as well as the growth of density perturbations. Although the potential of WL has been recognized for around two decades (e.g. [11]), only in the 1990s was there a surge of interest in this

area [12–17]. A unique property of WL is that it is sensitive directly to the amount of mass in the universe, avoiding the thorny issue of galaxy-to-mass bias. By measuring ellipticities of a large number of galaxies, one can in principle directly reconstruct the mass density field of an intervening massive object [18]. Indeed, the mass reconstruction of galaxy clusters has been successfully performed on a number of clusters (for a review, see Ref. [19]).

An exciting recent development, relevant to this work, was the discovery of weak lensing by large-scale structure, announced by four groups [20–23]. The results are in mutual agreement and consistent with theoretical expectations, which is remarkable given that they were obtained independently. Although current data impose weak constraints on cosmology (e.g., rule out the Einstein–de Sitter Universe with $\Omega_M=1$), future surveys with larger sky coverage and improved systematics are expected to impose interesting constraints on cosmological parameters.

The goal of this work is to assess the power of weak lensing to constrain dark energy. This analysis therefore complements that of Huterer and Turner [8], where the efficacy of SNe Ia and number-count surveys was considered. We follow the standard practice of considering dark energy to be a smooth component parametrized by its energy density (scaled to critical) Ω_X and equation-of-state ratio $w=p/\rho$ [24]. Dark energy modifies the WL observables by altering the distance-redshift relation and the growth of density perturbations. As discussed in Sec. VI B, the nonlinear evolution of perturbations also depends on dark energy; this dependence is much more difficult to calculate and needs to be calibrated from N -body simulations. Overall, the dependence of WL on dark energy is somewhat indirect and expected to be weak, especially when degeneracy with other cosmological parameters is taken into account. Nevertheless, we shall show that, provided systematic errors are controlled and theoretical predictions sharpened, WL surveys can be efficient probes of dark energy, comparable to SNe Ia and number-counts. Proposed deep wide-field surveys such

¹<http://snap.lbl.gov>

as LSST,² the aforementioned SNAP, and VISTA³ will attempt to constrain dark energy through their WL programs, making our analysis particularly timely.

Previous work on parameter determination from WL centered mostly on Ω_M and σ_8 , the rms density fluctuation in spheres of $8 h^{-1}$ Mpc [25,16]; here $H_0 = 100 h$ km/s/Mpc is the Hubble parameter today. Hu and Tegmark [26], however, used the Fisher matrix formalism to account for all 8 parameters upon which WL depends, and assumed dark energy to be the vacuum energy (therefore, fixed $w = -1$). We use the same set of parameters, with two changes: we add w , and, guided by the ever-stronger evidence from the cosmic microwave background (e.g., [27–30]), we assume a flat universe. To assess the accuracy of parameter determination, we too use the Fisher matrix machinery, which has proven to be an extremely efficient and accurate way to forecast errors in experiments where observables depend on many parameters.

This paper is organized as follows. In Sec. II we go over the basic formalism and define the notation. In Secs. III and IV we concentrate on the convergence power spectrum, and discuss its dependence on dark energy. Section V discusses the power of weak lensing surveys to probe dark energy, while Sec. VI addresses systematic errors that can lead to biases in parameter estimation. In Sec. VII we discuss the dependence of three-point statistics — bispectrum and skewness of the convergence — on dark energy. We conclude in Sec. VIII.

II. PRELIMINARIES

In this section we cover the basic formalism of weak gravitational lensing (for detailed reviews, see Refs. [31,19]). We work in the Newtonian gauge, where the perturbed Friedmann-Robertson-Walker metric reads

$$ds^2 = -(1 + 2\Phi)dt^2 + a^2(t)(1 - 2\Phi) \times [d\chi^2 + r^2(d\theta^2 + \sin^2\theta d\phi^2)] \quad (1)$$

where we have set $c = 1$, χ is the radial distance, Φ is the gravitational potential, and $k = 1, 0, -1$ for closed, flat and open geometry respectively. We also use the coordinate distance r which is defined as

$$r(\chi) = \begin{cases} (-K)^{-1/2} \sinh[(-K)^{1/2} \chi] & \text{if } \Omega_{\text{TOT}} < 1, \\ \chi & \text{if } \Omega_{\text{TOT}} = 1, \\ K^{-1/2} \sin(K^{1/2} \chi) & \text{if } \Omega_{\text{TOT}} > 1. \end{cases} \quad (2)$$

where K is the curvature, Ω_{TOT} is the total energy density relative to critical, and $K = (\Omega_{\text{TOT}} - 1)H_0^2$.

Gravitational lensing produces distortions of images of background galaxies. These distortions can be described as mapping between the source plane (S) and image plane (I) [32]

$$\delta x_i^S = A_{ij} \delta x_j^I \quad (3)$$

where $\delta \mathbf{x}$ are the displacement vectors in the two planes and A is the distortion matrix

$$A = \begin{pmatrix} 1 - \kappa - \gamma_1 & -\gamma_2 \\ -\gamma_2 & 1 - \kappa + \gamma_1 \end{pmatrix}. \quad (4)$$

The deformation is described by the convergence κ and complex shear (γ_1, γ_2) . We are interested in the weak lensing limit, where $|\kappa|, |\gamma| \ll 1$. The convergence in any particular direction on the sky $\hat{\mathbf{n}}$ is given by the integral along the line of sight,

$$\kappa(\hat{\mathbf{n}}, \chi) = \int_0^\chi W(\chi') \delta(\chi') d\chi', \quad (5)$$

where δ is the relative perturbation in matter energy density and

$$W(\chi) = \frac{3}{2} \Omega_M H_0^2 g(\chi)(1+z) \quad (6)$$

is referred to as the weight function. Furthermore

$$g(\chi) = r(\chi) \int_\chi^\infty d\chi' n(\chi') \frac{r(\chi' - \chi)}{r(\chi')} \quad (7)$$

$$\rightarrow \frac{r(\chi)r(\chi_s - \chi)}{r(\chi_s)} \quad (8)$$

where $n(\chi)$ is the distribution of source galaxies in redshift [normalized so that $\int dz n(z) = 1$] and the second line holds only if all sources are at a single redshift z_s . We use the distribution [20]

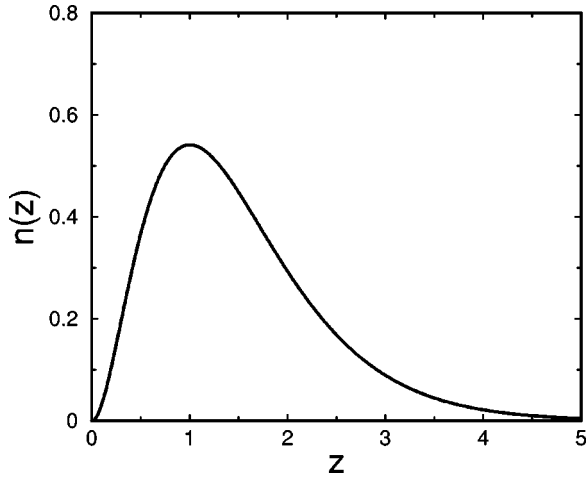
$$n(z) = \frac{z^2}{2z_0^3} e^{-z/z_0} \quad (9)$$

with $z_0 = 0.5$, which peaks at $2z_0 = 1$ and is shown in Fig. 1. Our results depend very weakly on the shape of the distribution of source galaxies (assuming this distribution is known, of course). In particular, if *all* source galaxies are assumed to be at $z = 1$, the parameter uncertainties change by at most $\sim 30\%$ percent. Similarly, the distribution given by Eq. (9) which peaks at $z = 1.5$ would improve the parameter constraints by 20% or less.

Some clarification is needed regarding observability vs. theoretical computability of WL quantities. The quantity that is most easily determined from observations is shear, which is directly related to the ellipticities of observed galaxies (in the weak lensing limit, shear is equal to the average ellipticity). Shear is given by [15]

²<http://dmtelescope.org>

³<http://www.vista.ac.uk>

FIG. 1. The assumed source galaxy distribution $n(z)$.

$$\gamma_1 + i\gamma_2 = \frac{1}{2}(\psi_{,11} - \psi_{,22}) + i\psi_{,12} \quad (10)$$

where ψ is the projected Newtonian potential, $\psi_{,ij} = -2\int g(\chi) \Phi_{,ij} d\chi$, and commas denote derivatives with respect to directions perpendicular to the line of sight. Unfortunately, this quantity is not easily related to the distribution of matter in the universe and the cosmological parameters. Convergence, on the other hand, is given by

$$\kappa = \frac{1}{2}(\psi_{,11} + \psi_{,22}) \quad (11)$$

which (in Limber's approximation) can be directly related to the distribution of matter through the Poisson equation [see Eq. (5)], and is convenient for comparison with theory. However, it is very difficult to measure the convergence itself, as convergence depends on the magnification of galaxies which would somehow need to be measured⁴ (although there may be ways to do this; see Ref. [33]). Note also that computing the convergence from the measured shear is difficult in general, since the inversion kernel is broad and requires knowledge of shear everywhere [18]. In the weak lensing limit, however, the problem is much easier, since the two-point correlation functions of shear and convergence are identical.

In this work we use power spectrum of the convergence [defined in Eq. (13) below] as the principal observable that will convey information from weak lensing.

III. CONVERGENCE POWER SPECTRUM

The convergence can be transformed into multipole space (see e.g. Ref. [31])

⁴There are two competing effects due to magnification of galaxies: (1) "Magnification bias," the increase in the observed number of galaxies due to the fact that fainter ones can not be observed, and (2) increase in the apparent observed area on the sky due to lensing, which decreases the observed number density of galaxies.

$$\kappa_{lm} = \int d\hat{\mathbf{n}} \kappa(\hat{\mathbf{n}}, \chi) Y_{lm}^*$$

The power spectrum of the convergence P_l^κ is then defined by

$$\langle \kappa_{lm} \kappa_{l'm'} \rangle = \delta_{l_1 l_2} \delta_{m_1 m_2} P_l^\kappa.$$

Using Limber's approximation — the fact that the weight function W is much broader than the physical scale on which the perturbation δ varies — the convergence power spectrum can be written as

$$P_l^\kappa = \int_0^{\chi_s} d\chi \frac{W^2(\chi)}{r^2(\chi)} P(l/r(\chi), z) \quad (12)$$

$$= \frac{2\pi^2}{l^3} \int_0^{z_s} dz \frac{W^2(z)r(z)}{H(z)} \Delta^2(l/r(z), z) \quad (13)$$

where in the second line we assume a flat universe where $d\chi = dr$. Here $P(k, z)$ is the matter power spectrum as a function of redshift z , and

$$\Delta^2(k, z) = \frac{k^3 P(k, z)}{2\pi^2} \quad (14)$$

is power per unit logarithmic interval in wavenumber, which we also refer to as the matter power spectrum.

Power spectrum of the convergence is displayed in the top panel of Fig. 2 for three values of (Ω_X, w) and down to scales of about one arcminute ($l = 10000$). The uncertainty in the observed weak lensing spectrum is given by [14,15]⁵

$$\Delta P_l^\kappa = \sqrt{\frac{2}{(2l+1)f_{\text{sky}}}} \left(P_l^\kappa + \frac{\langle \gamma_{\text{int}}^2 \rangle}{n} \right), \quad (15)$$

where $f_{\text{sky}} = \Theta^2 \pi / 129600$ is the fraction of the sky covered by a survey of dimension Θ and $\langle \gamma_{\text{int}}^2 \rangle^{1/2} \approx 0.4$ is the intrinsic ellipticity of galaxies. The first term corresponds to cosmic variance which dominates on large scales, and the second to Poisson noise which arises due to small number of galaxies on small scales. Bottom panel of Fig. 2 shows the signal-to-noise $P_l^\kappa / \Delta P_l^\kappa$. It is apparent that the bulk of cosmological constraints comes from multipoles between several hundred and several thousand. Wider and deeper surveys widen the range of scales with high signal-to-noise. Note also that the weak lensing power spectrum is relatively featureless because of the radial projection [Eq. (13)]. It can be characterized by amplitude (normalization), overall tilt, a "turnover" at $l \sim 100$ which is due to the turnover in the matter power spectrum, and a further increase at $l \sim 1000$ and flattening at $l \sim 10000$ which are due to the nonlinear clustering of matter.

⁵Strictly speaking, Eq. (15) holds for Gaussian convergence field only. However, the non-Gaussianity of the convergence is milder than that of the matter due to the radial projection which makes this a good approximation, see Sec. VI C.

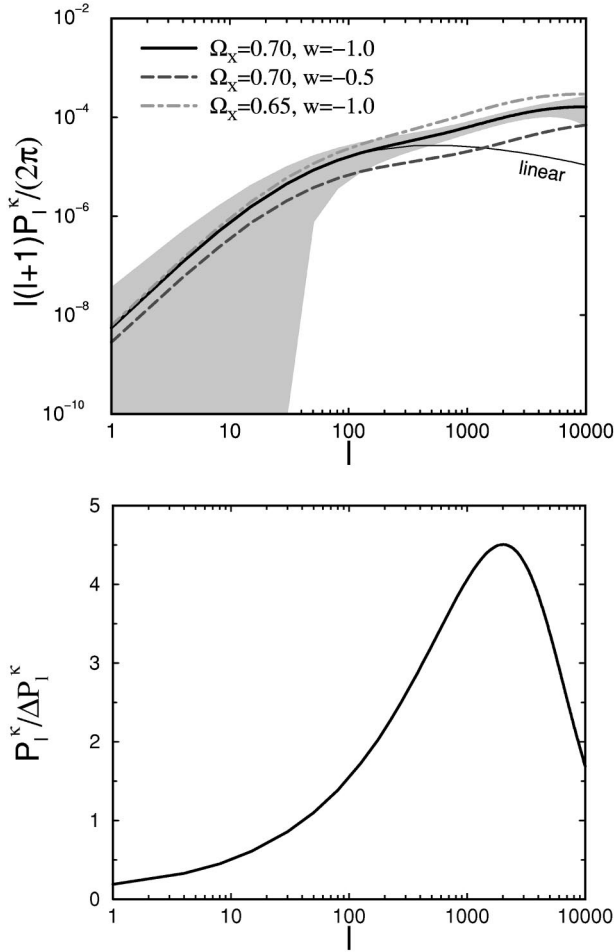


FIG. 2. *Top panel:* The convergence power spectrum for three pairs of (Ω_X, w) . The shaded region represents 1σ uncertainties (corresponding to $\Omega_X=0.7, w=-1$ curve) plotted at each l . The uncertainties at low l are dominated by cosmic variance, and those at high l by Poisson (shot) noise; see Eq. (15). We also show the contribution to P_l^kappa from the *linear* matter power spectrum only. *Bottom panel:* $P_l^kappa/\Delta P_l^kappa$ (“signal-to-noise”) for the convergence power spectrum for each individual l .

The systematic error in shear measurements ideally needs to be small enough so as not to exceed the statistical error shown in Fig. 2. The maximum allowed systematic error can be estimated using the following argument.⁶ The shear variance in circular aperture of opening angle θ can be written in terms of the convergence power spectrum as [31]

$$\langle \gamma^2(\theta) \rangle = 2\pi \int_0^\infty dl l P_l^kappa \left(\frac{J_1(l\theta)}{\pi l \theta} \right)^2 \quad (16)$$

$$\approx (2\pi)^2 \int_0^\infty \frac{dl}{l} \mathcal{P}_\kappa^l \left(\frac{J_1(l\theta)}{\pi l \theta} \right)^2 \quad (17)$$

$$\approx \mathcal{P}_\kappa^{l=1/\theta} \quad (18)$$

which is the power in unit logarithmic interval evaluated at $l=1/\theta$ [here $\mathcal{P}_\kappa^l = l(l+1)/(2\pi)P_l^kappa$]. The tightest requirement is on scales of 1 arcmin ($l \approx 2000$), where the fractional uncertainty in power per unit logarithmic interval is about $1/200$. Therefore the rms of shear on scale θ is given by

$$\delta \sqrt{\langle \gamma^2(\theta) \rangle} \approx \delta \sqrt{\mathcal{P}_\kappa^{l=1/\theta}} \quad (19)$$

$$= \frac{1}{2} \sqrt{\mathcal{P}_\kappa^{l=1/\theta}} \left(\frac{\delta \mathcal{P}_\kappa^{l=1/\theta}}{\mathcal{P}_\kappa^{l=1/\theta}} \right) \quad (20)$$

$$\approx \frac{1}{2} \times \sqrt{10^{-4}} \times \frac{1}{200} \quad (21)$$

$$\approx 2.5 \times 10^{-5} \quad (22)$$

$$\leq 0.01 \sqrt{\langle \gamma^2(\theta) \rangle}. \quad (23)$$

Therefore, the systematic error in individual shear measurements should be less than 1% in order to be subdominant to statistical error—a very challenging requirement indeed.

IV. DEPENDENCE ON DARK ENERGY

The sensitivity of the convergence power spectrum to dark energy can be divided into two parts. Dark energy (a) modifies the background evolution of the universe, and consequently the geometric factor $W^2(z)r(z)/H(z)$, and (b) modifies the matter power spectrum. We now discuss each of these dependencies.

A. The lensing weight function

Function $W(z)$ is bell-shaped, and has a maximum at $z \approx z_s/2$, where z_s is redshift of lensed galaxies, indicating that lensing is the most effective at distances halfway between the source and the observer. Since $r(z)$ and $H(z)$ are varying with redshift monotonically and slowly, the function $W^2(z)r(z)/H(z)$ will also be bell-shaped with maximum at $z \gtrsim z_s/2$. $W(z), r(z)$ and $1/H(z)$ all decrease with increasing w , and therefore the total weight decreases. As Ω_X decreases, $r(z)$ and $1/H(z)$ decrease but $W(z)$ increases, and the latter prevails; see Fig. 3. Therefore, changing $w(\Omega_X)$ makes the normalization and total weight change with the same (opposite) sign, leading to large (small) change in P_l^kappa on large scales; see Fig. 2.

B. The matter power spectrum

The matter power spectrum can be written as

$$\Delta^2(k, z) = \delta_H^2 \left(\frac{k}{H_0} \right)^{3+n} T^2(k, z) \frac{D^2(z)}{D^2(0)} T_{NL}(k, z) \quad (24)$$

where δ_H is perturbation on Hubble scale today, $T(k)$ is the transfer function, $D(z)/D(0)$ is the growth of perturbations in linear theory relative to today, and $T_{NL}(k, z)$ is the prescription for nonlinear evolution of the power spectrum.

⁶Proposed by M. Turner.

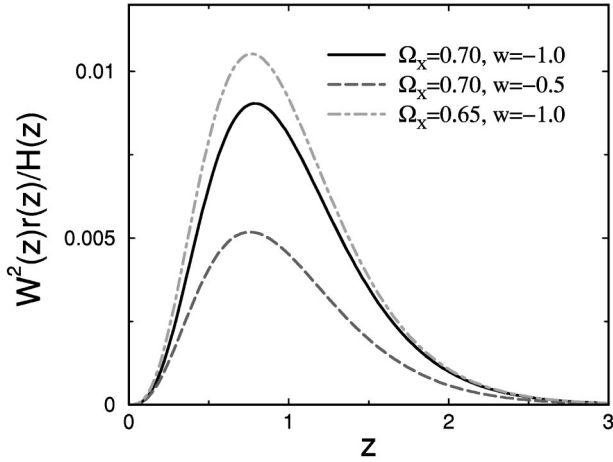


FIG. 3. The weight function $W^2(z)r(z)/H(z)$ for three pairs of (Ω_X, w) .

In the presence of dark energy, the matter power spectrum will be modified as follows.

The normalization δ_H increases with increasing Ω_X and decreasing w . This happens because the growth of structure is suppressed in the presence of dark energy, and the observed structure today can only be explained by a larger initial amount of perturbation. We choose to normalize the results to Cosmic Background Explorer (COBE) measurements [34], and adopt the fit to COBE data of Ma *et al.* ([35], heretofore Ma QCDM)

$$\delta_H = 2 \times 10^{-5} \alpha(0)^{-1} \Omega_M^{c_1 + c_2 \ln(\Omega_M)} \times \exp[c_3(n-1) + c_4(n-1)^2] \quad (25)$$

where $c_1 \dots c_4$ and α_0 are functions of Ω_X and w and are given in Ma QCDM. Since the COBE normalization for the Λ CDM models is accurate to between 7% and 9% [36,37], we adopt the accuracy of 10% for the dark-energy case.

The transfer function for cosmological models with neutrinos and the cosmological constant is given by fits of Hu and Eisenstein [38], which we adopt in our analysis. These formulas are accurate to a few percent for the currently favored cosmology with low baryon abundance. Dark energy will not directly modify the transfer function, except possibly on the largest observable scales (of size $\sim H_0^{-1}$), where dark energy may cluster. This signature can be ignored, as it shows up on scales too large to be probed by WL; we further discuss this in Sec. V G.

The linear theory growth function $D(z) = \delta(z)/\delta(0)$ can be computed from the fitting formula for the dark-energy models given in Ma QCDM, which generalizes the Λ CDM growth function formula of Carroll *et al.* [39]. We use this fitting function, noting that its high accuracy ($\leq 2\%$) justifies avoiding the alternative of repeatedly evaluating the exact expression for the growth function (e.g. [40], p. 341).

The last, and most uncertain, piece of the puzzle is the prescription for the non-linear evolution of density perturbations. This is given by the recipe of Hamilton *et al.* [41] as

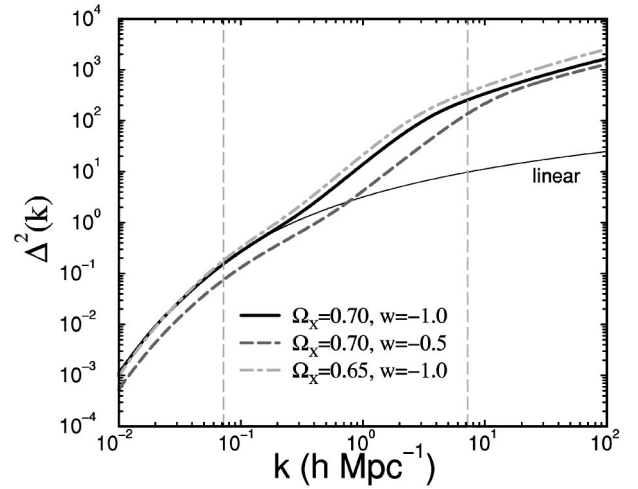


FIG. 4. The matter power spectrum at $z=0$ for three pairs of (Ω_X, w) . Linear power spectrum corresponding to the fiducial spectrum is shown by the thin solid curve. Vertical lines delimit the interval which contributes significantly to the WL convergence power spectrum, roughly corresponding to $100 \leq l \leq 10000$. It can be seen that the ability to determine cosmological parameters will depend critically upon the knowledge of the nonlinear power spectrum.

implemented by Peacock and Dodds [42]; (PD), as well as Ma ([43], heretofore Ma Λ CDM). These two prescriptions were calibrated for Λ CDM models, although the PD formula seems to adequately fit models with $w > -1$ [M. White (private communication)]. Ma QCDM prescription [35], on the other hand, gives explicit formulas for the nonlinear power spectrum in the presence of dark energy (i.e., a component with $w \geq -1$). Unfortunately, we found that the PD and Ma QCDM prescriptions agree (to $\sim 15\%$) only at values of w where Ma QCDM was tested. At other values of w the maximum disagreement between the two is up to 50%, and it is not clear which fitting function, if any, is to be used. We choose to use the PD prescription primarily because it is implemented for all w and therefore facilitates taking the derivative with respect to w needed for the Fisher matrix. In Sec. VI B we explore the possible parameter biases due to the uncertain calibration of the nonlinear power spectrum.

Figure 4 shows the matter power spectrum at $z=0$ for three pairs of (Ω_M, w) . When Ω_X or w are varied, the growth and normalization change affecting all scales equally. Varying Ω_X also changes the transfer function (at $k \gtrsim 0.02 h^{-1}$ Mpc). On smaller scales ($k \gtrsim 0.2 h^{-1}$ Mpc), the non-linear power spectrum is further affected by dark energy.

C. Angular scale–physical scale correspondence

To illustrate the correspondence between wave numbers k and multipoles l , let us assume the matter power spectrum peaked at a single multipole k_1

$$\Delta^2(k) = \langle \delta^2 \rangle k_1 \delta(k - k_1) \quad (26)$$

normalized so that $\int \Delta^2(k) d \ln k = \langle \delta^2 \rangle$ (here $\langle \delta^2 \rangle$ is the auto-

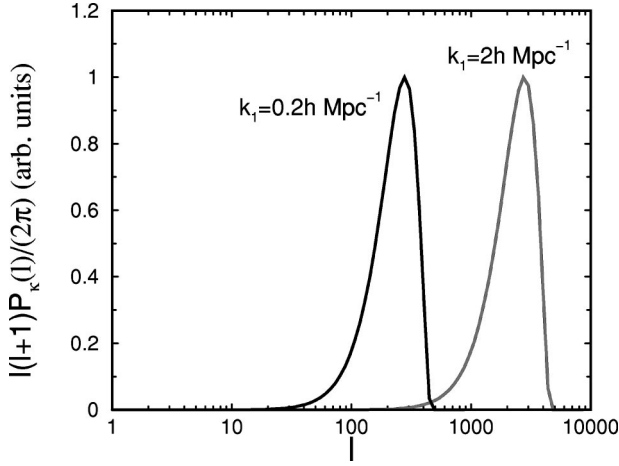


FIG. 5. Power spectrum of the convergence assuming matter power spectrum is a delta-function at k_1 , shown for two different values of k_1 . This shows the correspondence between physical and angular scales (for $z_s=1$ and our fiducial Λ CDM cosmology).

correlation function of density contrast in real space). Then, assuming for simplicity that all sources are at a single redshift z_s , we have

$$l(l+1)P_l^\kappa/(2\pi) \propto \frac{l^3}{k_1^4} \left(1 - \frac{l}{r(z_s)k_1}\right)^2 \quad (27)$$

for $l < k_1 r(z_s)$, and zero for $l \geq k_1 r(z_s)$. The plot of the convergence power spectrum is given in Fig. 5 for two values of k_1 . The multipole power peaks at $l = 3/5 k_1 r(z_s)$. Assuming a survey with $z_s = 1$, the scale at which the non-linear effects become significant, $k \approx 0.2 h^{-1} \text{ Mpc}$, corresponds to $l \approx 300$. Our constraints mostly come from angular scales $l \sim 1000$, corresponding to $k \sim 1 h^{-1} \text{ Mpc}$. The bulk of WL constraints therefore comes from non-linear scales.

V. CONSTRAINTS ON DARK ENERGY

A. The Fisher matrix formalism

The fact that the relatively featureless P_l^κ depends upon a number of cosmological parameters directly leads to parameter degeneracies and limits the power of weak lensing to measure these parameters independently of other probes, even for the case of a full-sky survey. To estimate how accurately cosmological parameters can be measured, we use the Fisher matrix formalism [44]. This method has already been used to forecast the expected accuracies from CMB surveys [45,46], SNe Ia [47,8,6] and number counts [48] and was found to agree very well with direct Monte Carlo error estimation. Its considerable advantage over Monte Carlo calculation is that it does not require simulations and analyses of data sets, but only a single evaluation of a simple analytic expression. Furthermore, the Fisher matrix formalism allows easy inclusion of Bayesian priors and constraints from other methods.

The Fisher matrix is defined as the second derivative of the negative log-likelihood function

$$F_{ij} = - \left\langle \frac{\partial^2 \ln L}{\partial p_i \partial p_j} \right\rangle_{\mathbf{x}} \quad (28)$$

$$= \sum_l \frac{1}{(\Delta P_l^\kappa)^2} \frac{\partial P_l^\kappa}{\partial p_i} \frac{\partial P_l^\kappa}{\partial p_j} \quad (29)$$

where L is the likelihood of the observed data set \mathbf{x} given the parameters $p_1 \dots p_n$. The second line follows by assuming that L is Gaussian in the observable P_l^κ , which is a good assumption for small departures around the maximum.

In practice we do not estimate the power spectrum at every multipole l , but rather bin P_l^κ in 17 bins. We explicitly checked that binning makes no significant difference in our results (this is not surprising, as the convergence power spectrum does not have features that would get washed out by moderate-resolution binning). We considered P_l^κ at $100 \leq l \leq 10000$, corresponding to angles between 1 arcmin and 2° on the sky. Variations in the minimum and maximum l do not change any of our results, as very large and very small scales are dominated by cosmic variance and Poisson noise respectively.

Finally, we need to choose steps in parameter directions when taking numerical derivatives. We choose the steps to be 5% of the parameter values, making sure to take two-sided derivatives.

B. The fiducial cosmology and fiducial survey

Finally, we need to choose the fiducial survey, i.e. sky coverage and depth of the survey. We do not consider any single experiment in particular, but rather adopt numbers roughly consistent with proposed dedicated wide-field surveys expected to become operational in several years. We assume a survey covering 1000 sq deg down to a limiting magnitude $R=27$; dependence of the results upon these two parameters is discussed in Sec. V F. Surveys of this power are not yet operational, but are expected in the near future with results perhaps by the end of this decade. To convert from magnitudes to surface density of galaxies, we use the correspondence from Herschel and Hubble Deep Fields [49], which for our fiducial numbers implies 165 gal/arcmin². We assume that the *only* sources of noise are statistical: cosmic variance which dominates on large scales, and shot-noise dominant on small scales. We discuss the effect of systematics in Sec. VI.

C. Parameter space

Power spectrum of the convergence depends on 7 parameters: $\Omega_X, w, \Omega_M h^2, \Omega_B h^2, \delta_H, n$, and m_ν , where Ω_B is the energy density in baryons (relative to critical), n is the spectral index of scalar perturbations, and m_ν the neutrino mass summed over all species. In addition, P_l^κ depends upon the redshift distribution of source galaxies. Throughout, we use a fiducial model that fits well all experiments so far: $\Omega_X = 1 - \Omega_M = 0.7$ (flat universe assumed), $h = 0.65, \Omega_B h^2 = 0.019, n = 1.0$, and δ_H inferred from COBE measurements as described in Sec. IV B. The mass of neutrino species is

quite uncertain, but, according to solar neutrino experiments, likely to be between zero and a few eV; we adopt $m_\nu = 0.1$ eV.

We would like to get an insight in parameter degeneracies, in particular between the equation of state ratio w and other parameters. To do that, we compute the correlation between w and other parameters. The correlation coefficient is given by

$$\rho(w, p_i) = \frac{\text{Cov}(w, p_i)}{\sqrt{\text{Cov}(w, w)\text{Cov}(p_i, p_i)}} \quad (30)$$

where $\text{Cov}(p_i, p_j) = F_{ij}^{-1}$ is an element of the covariance matrix. Because imposing priors would alter the covariance matrix and confuse its interpretation, at this point we add no priors except for COBE normalization (10% in δ_H) and perfect knowledge of galaxy redshifts.

The most significant correlations are $\rho(w, \Omega_X) = -0.96$, $\rho(w, \Omega_B h^2) = -0.83$, and $\rho(w, m_\nu) = 0.81$. We find that these and other correlations are typically very dependent on the fiducial model and the assumed prior. Finally, we examine the eigenvalues and eigenvectors of the Fisher matrix. The combination $0.61 \Omega_X + 0.21 w$ is determined to an accuracy of about 0.03; this is the best-determined combination containing significant components in Ω_X and w directions. The least well determined combination of all is one almost entirely in the w -direction: $0.97 w - 0.21 \Omega_X$; it is determined to about 0.4.

D. Bayesian priors

Without *any* prior information on cosmological parameters, weak lensing imposes very weak constraints on dark energy (and other parameters as well). The reason is that the power spectrum of the convergence is featureless, owing to the fact that it represents the radial projection of the density contrast. Unlike the CMB spectrum, it lacks bumps and wiggles that would help break parameter degeneracies. Constraints rapidly improve, however, if the redshift distribution of source galaxies is known. We assume this to be the case; indeed, photometric redshift techniques already show that distribution of source galaxies in weak lensing surveys will be determined independently of cosmological parameters (e.g., [50]). Exact knowledge of the source distribution is obviously a strong and perhaps unrealistic assumption, and in Sec. VI we explore what happens when the uncertainties are included.

There is no reason to expect that any cosmological probe alone should carry the burden of determining all cosmological parameters. Indeed, a number of cosmological parameters are already pinned down quite accurately by other means. In about 10 years, when powerful weak lensing surveys we consider complete their observational programs, parameters inferred from the CMB (such as $\Omega_M h^2$, $\Omega_B h^2$ and n) will be determined to an accuracy of several percent [46]. The neutrino mass, on the other hand, is poorly known today, but in the near future it is likely to be constrained by a combination of CMB, Ly- α forest [51], as well as solar and atmospheric neutrino measurements.

For these reasons, we include Gaussian priors on cosmological parameters (other than Ω_X and w). We consider two sets of priors, and call them ‘‘COBE+photo-z’’ and ‘‘Planck (T).’’ The former set of priors is a weak one: we only include the 10% uncertainty in COBE normalization and, as mentioned above, knowledge of the distribution of background galaxies. The latter set is a moderate one, corresponding to the COBE+photo-z prior, plus the constraints expected from the Planck mission with temperature information only (Table 2 of Ref. [46]): $\sigma(\ln \Omega_M h^2) = 0.064$, $\sigma(\ln \Omega_B h^2) = 0.035$, $\sigma(n) = 0.04$, and $\sigma(m_\nu) = 0.58$.⁷ We note, however, that details of the second prior do not change the results much; for example, using the considerably weaker assumptions corresponding to Microwave Anisotropy Probe (MAP) mission (with temperature only) instead of Planck (T), errors in Ω_X and w degrade by only 10% and 5% respectively. Similarly, using the very strong prior of Planck constraints (temperature and polarization) combined with those from Sloan Digital Sky Survey (SDSS⁸), the constraints improve only by about 20%. The reason for this weak dependence on the prior is easy to understand: by assuming the knowledge of the distribution of source galaxies and adding other priors, we have broken the major degeneracy between Ω_X, w and other parameters; further information on other parameters leads to small improvements in the constraints on dark energy.

E. Results

An example of the constraints that weak lensing can impose on dark energy is shown in Fig. 6. Here we show the 68% constraint regions for our fiducial WL survey (1000 sq deg down to 27th mag) with several sets of priors on other parameters. The ellipse is oriented so that increase in w is degenerate with increase in Ω_M , which is opposite of what we would expect; this is due to the fact that we assume galaxy redshifts to be known.⁹ Table I lists the uncertainties using two sets of priors. Weak lensing is potentially a strong probe of dark energy: the 1σ uncertainties in Ω_X and w are $\sim 5\%$ and 20–40 % respectively (depending on the set of priors), which is somewhat weaker than statistical errors expected from future SNe Ia and number-count surveys. We emphasize that these numbers are the best ones possible given the survey specifications; systematic errors may weaken the constraints (see Sec. VI). It is also true, however, that weak lensing tomography can significantly *improve* these constraints (more on that in Sec. V F).

Left panel of Fig. 7 shows the dependence of the uncertainties in Ω_X and w on the sky coverage, holding the depth

⁷Strictly speaking, the correct way to add the CMB priors would be to add the WL and CMB Fisher matrices. This procedure would correctly account for breaking of the WL parameter degeneracies by the CMB. We opt, however, to just add the priors to the diagonal elements of the WL Fisher matrix. This effectively assumes other parameters to be constrained within some limits, regardless of what experiment those constraints come from.

⁸<http://www.sdss.org>

⁹In general, priors on other cosmological parameters will change the orientation of the constraints in the Ω_M - w plane.

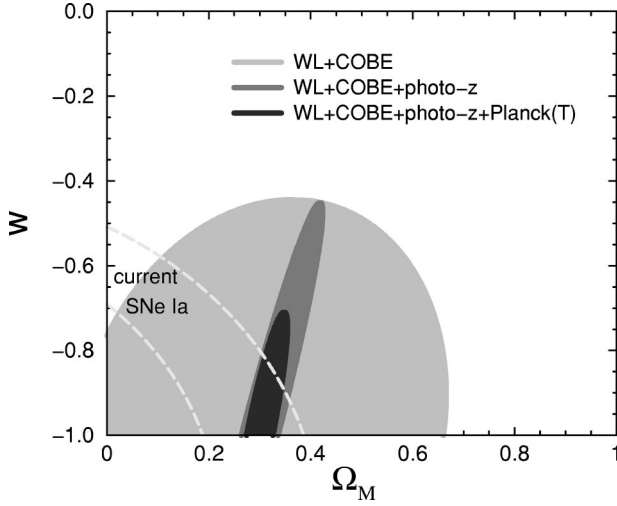


FIG. 6. 68% C.L. constraints on Ω_M and w for three different priors on other parameters. We assume a survey of 1000 sq deg down to 27th magnitude in R -band, and assume knowledge of the distribution of source galaxies. The strength of the constraints does not depend sensitively on the set of priors, but does depend on the fiducial model (e.g., the neutrino mass). For orientation, current 1σ constraints from 42 type Ia supernovae [2] are also shown.

of the survey fixed at 27th mag. Right panel of the same figure shows dependence of the uncertainties on the depth of the survey, holding the sky coverage fixed at 1000 sq deg. The constraints on w depend quite strongly on the depth of the survey — for example, constraint on w would improve by a factor of two by increasing the coverage of the survey to 5000 sq deg. The dependence on the depth is also significant, but probably complicated by some practical problems; for example, galaxy overlap. Therefore, future surveys with very deep and/or wide sky coverage will be especially effective probes of dark energy.

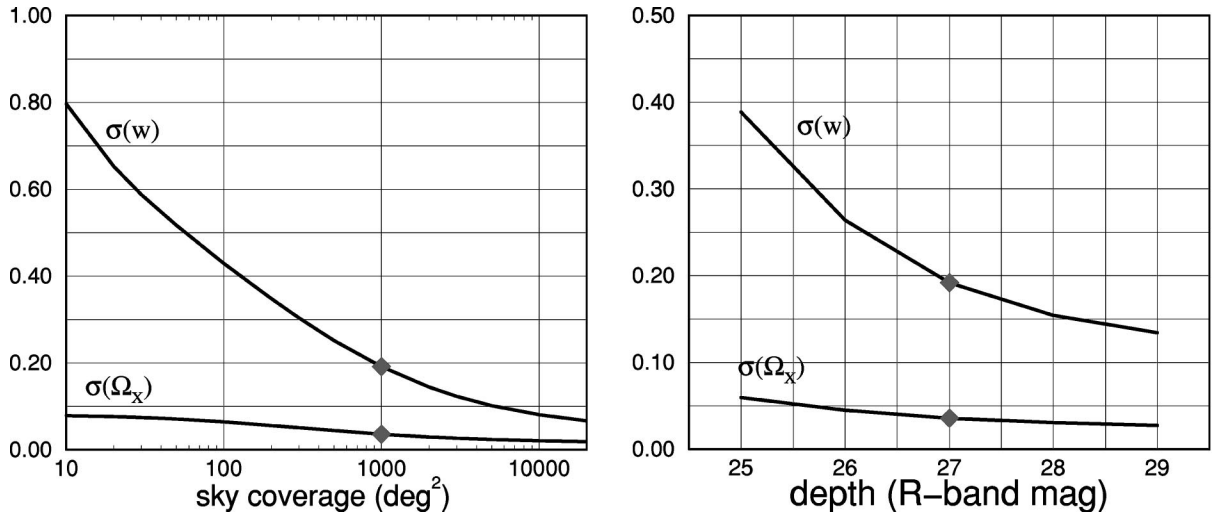


FIG. 7. Dependence of $\sigma(\Omega_X)$ and $\sigma(w)$ on the survey parameters. In each case we assume Planck (T) priors on other cosmological parameters. Diamonds denote the fiducial values. *Left panel*: 1σ uncertainties on Ω_X and w as a function of sky coverage of the survey. We assume a fixed depth of 27th magnitude in R -band. *Right panel*: 1σ uncertainties on Ω_X and w as a function of depth of the survey, assuming a fixed sky coverage of 1000 sq deg.

TABLE I. Constraints on dark energy.

	Prior	
	COBE + photo-z	Planck (T)
$\sigma(\Omega_X)$	0.08	0.04
$\sigma(w)$	0.36	0.19

F. Power spectrum tomography

One way to extract more information out of the data would be to divide the lensed galaxies in several redshift bins and measure the convergence power spectrum in each bin, as well as the cross power spectrum between bins. This procedure, the power spectrum tomography, should be fully feasible with upcoming surveys because redshifts of source galaxies are going to be known quite accurately through photometric techniques. Following the formalism of Hu [52], we compute the parameter constraints when source galaxies are separated in redshift. Of the several slicings in two bins we tried, the most effective division was below and above $z = 1.0$ (Fig. 8, left panel). In this case, the constraints on Ω_X and w improve by a factor of 3 and 1.4 respectively, for a Planck(T) prior (Fig. 9). For the weaker COBE+photo-z prior, the improvement is even more significant: a factor of 5 and 3 improvements on Ω_X and w respectively.

We also consider an optimistic scenario where galaxies can be separated in 10 redshift bins (Fig. 8, right panel). Whether or not and how accurately something like this can be done using photometric redshift techniques is presently under investigation [Eisenstein, Hu, and Huterer (in preparation)]. The constraints on Ω_M (or Ω_X) and w further improve: $\sigma(\Omega_X) = 0.012$ and $\sigma(w) = 0.07$ (Fig. 9).

Subdividing the galaxy population in more than two redshift bins leads to fairly limited improvements in parameter determination; this is due to high correlations ($\sim 80\%$) between the power spectra in different bins [52]. Nevertheless,

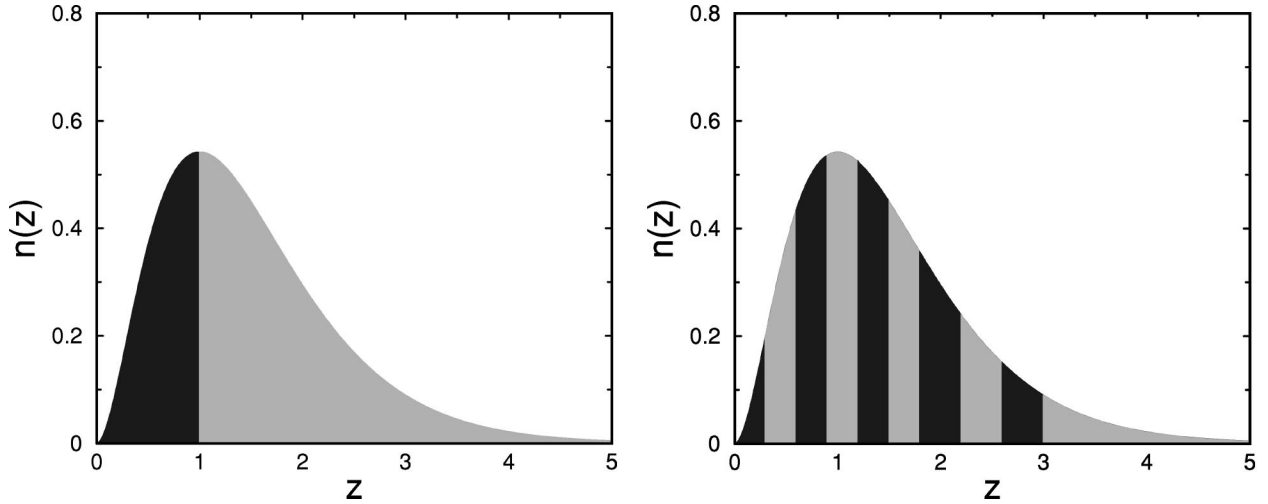


FIG. 8. The divisions of source galaxies in redshift we used in order to implement the tomography. *Left panel:* A simple division in two redshift bins. *Right panel:* A division in 10 redshift bins.

tomography clearly adds valuable information on cosmological parameters and should be pursued with data from future WL experiments. In order to accurately assess and optimize this technique, further study considering realistic accuracy of photometric redshifts is necessary. Using simplified assumptions (in particular, no “leakage” of galaxies between bins), we have shown here that separation of galaxies in redshift easily leads to a factor of a few improvement in measuring Ω_X and w .

We now discuss whether a specific signature of certain dark-energy models can be detected with WL surveys.

G. Detecting the dark-energy clustering?

Evolving scalar fields, or quintessence, are a particular class of candidates for dark energy (e.g. [53–55]). One signature of quintessence is that it generally clusters around and

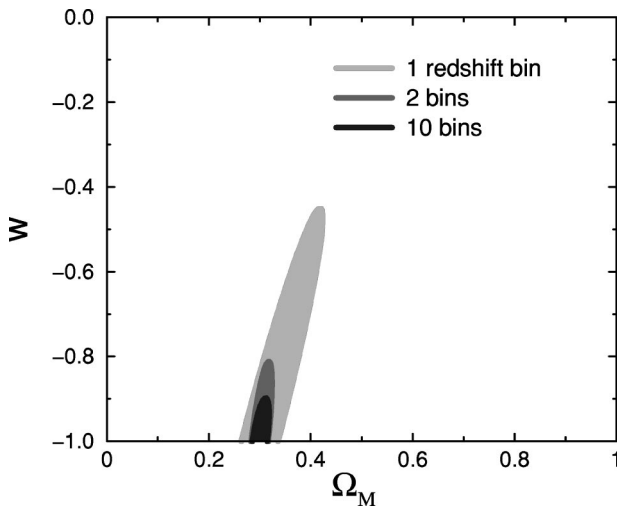


FIG. 9. The improvement in the constraint on Ω_M and w due to tomography. The 68% C.L. constraint regions correspond to 1, 2 and 10 divisions in redshift (largest to smallest ellipse), and are all computed using the COBE + photo- z prior.

above the Hubble radius scale H_0^{-1} . We ask: is it possible to detect this clustering in wide-field weak lensing surveys?

The clustering of quintessence is reflected in the increase in the transfer function on very large scales. The effect is more pronounced for larger Ω_X and larger w , and explicit forms for $T_Q(k, z)$ are given in Refs. [35] and [56]; here T_Q is the transfer function that takes clustering into account. Clustering changes the matter power spectrum on large scales, which in turn alters the convergence power spectrum at lowest multipoles. In Fig. 10 we show an optimistic scenario¹⁰ with $w = -1/3$ with and without clustering taken into account. We used exact formulas for the convergence power spectrum [57], since Limber’s approximation breaks down at lowest multipoles. Even though the effect on the matter power spectrum is significant [$T_Q(k, z)/T_\Lambda(k, z) \approx 2.0$ at $k \sim H_0$ in this case], the convergence power spectrum changes noticeably only at $l = 1$, and even there only by $\sim 30\%$. As this figure shows, the effect is buried deeply in the cosmic variance even for a full-sky WL survey. Therefore, it is unlikely that WL alone can detect the clustering of quintessence. However, cross correlation of WL and other methods (e.g. the CMB) may be more promising; see Refs. [58,59].

VI. SYSTEMATICS AND BIASES

A. Observational issues

It is difficult to overemphasize the importance of controlling the various systematic errors that generically creep into the WL observing process. These include shear recovery issues, anisotropic point-spread function, the quality of seeing, and instrumental noise (for a nice study of systematic effects, see Ref. [60]). There is also the effect of overlapping galaxies, which is expected to be especially pronounced in very deep surveys, but might be overcome using the photometric

¹⁰In a sense that a more positive w leads to more clustering.

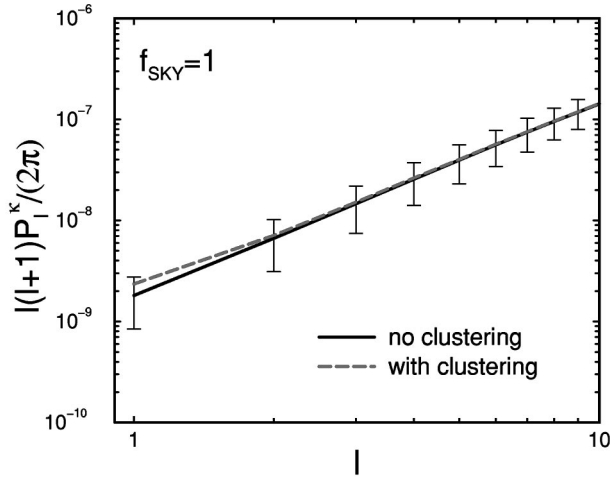


FIG. 10. The effect of clustering of quintessence on the convergence power spectrum for a fiducial equation-of-state ratio $w = -1/3$. The error bars correspond to the cosmic variance for a full-sky weak lensing survey. Clustering affects the $l=1$ multipole the most, but even there the effect is buried within cosmic variance.

redshift information [M. Joffe (private communication)]. Finally, the observed galaxies might be intrinsically aligned due to coupling of their angular momenta or a similar mechanism ([61–63] and references therein); this has already been observed [64,65]. These effects may masquerade as the signal itself, and make the extraction of ellipticity correlations very difficult. In our analysis, we have assumed that these problems will be resolved, and that the dominant uncertainty will be the cosmic variance on large scales and Poisson noise on small scales. In that sense, our results (for a given parameter space, set of priors, and fiducial survey strategy) may be optimistic. On the other hand, rapid advances in our understanding of weak lensing techniques, as well as the prospects of powerful future surveys, indicate that in a few years we can expect a much better understanding of the aforementioned problems.

B. Dependence upon nonlinear power spectrum and galaxy distribution

In addition to observational systematics that need to be controlled, theoretical prediction for the angular power spectrum of the convergence is also uncertain. Uncertainties in the nonlinear matter power spectrum (NLPS) and in the redshift distribution of galaxies are especially significant, as they are difficult to quantify and were not included in our analysis. We now discuss these two ingredients in more detail.

As can be seen from Figs. 2 and 4, most of our constraints come from nonlinear scales. Therefore, knowledge of the NLPS is crucial in order to compare experimental results with theory. However, this quantity is perhaps the most uncertain ingredient in the prediction for the power spectrum of the convergence. The NLPS is traditionally obtained by running N -body simulations for several cosmological models and deriving a fitting function to the simulated nonlinear power spectra. For the models with dark energy we consider,

TABLE II. Parameter biases.

p_i	Due to “wrong” NLPS		Due to “wrong” $n(z)$	
	bias	bias / $\sigma(p_i)$	bias	bias / $\sigma(p_i)$
Ω_X	0.09	2.5	0.04	1.2
w	0.92	4.8	0.57	3.0

either PD or Ma QCDM fitting functions can be used. The latter was calibrated for quintessence models in a flat universe, and tested at $w = -2/3, -1/2$ and $-1/3$ and $\Omega_M = 0.4$ and 0.6.

Even with this solution, the intrinsic uncertainty of 5–15% in the NLPS is significant (recall, the transfer and growth functions are accurate to just a few percent). To illustrate the importance of knowing the NLPS accurately, let us for the moment *assume* that the true NLPS at $w = -1$ is that given by the formula of PD. Let us further *assume* that, not knowing this, we adopt the Ma QCDM prescription to compute the theoretical power spectra. We now compute the bias in cosmological parameters due to this “erroneous” assumption. Let us write the cosmological parameter values as

$$p_i = \bar{p}_i + \delta p_i \quad (31)$$

where \bar{p}_i is the true value, p_i the measured value, and δp_i the bias due to using the “wrong” NLPS. Assuming that these biases are small, it is easy to show that [66]

$$\delta p_i = F_{ij}^{-1} \sum_l \frac{1}{(\Delta P_l^\kappa)^2} (P_l^\kappa - \bar{P}_l^\kappa) \frac{\partial \bar{P}_l^\kappa}{\partial p_j} \quad (32)$$

where F_{ij} is the ubiquitous Fisher matrix, $P_l^\kappa(\bar{p}_l^\kappa)$ is the “erroneous” (“true”) power spectrum, and sum over j is implied. The results of this exercise are given in Table II where we consider our fiducial survey with Planck (T) prior. The biases in Ω_X and w are 2.5 and 4.8 times the 1σ uncertainties in these parameters. Even though these numbers may not be accurate because the approximation $\delta p \ll \bar{p}$ necessary to use Eq. (32) obviously did not hold, one can still conclude that the biases are very significant. Therefore, we need a more accurate knowledge of the NLPS.

Fortunately, the NLPS obstacle is surmountable. It is a matter of running powerful N -body simulations that include dark energy, on a fine grid in w (and m_ν and other parameters, if necessary). Because we are only interested in the matter power spectrum (not galaxy power spectrum, which includes bias), N -body simulations can in principle give the NLPS to a very high accuracy. Once this is achieved, weak lensing will regain much of its power to probe dark energy.

Another quantity that may not be known to an extremely high accuracy (although we assumed so) is the redshift distribution of source galaxies $n(z)$. Indeed, current photometric redshift techniques can determine redshifts to an accuracy of ~ 0.1 , depending on the redshift (e.g., [50]), which leaves room for error, both statistical and systematic. To include the uncertainty in $n(z)$, some authors (e.g., [16,25,26]) param-

etrized the redshift distribution by one parameter only. However, the realistic uncertainty in $n(z)$ is much more difficult to quantify. To assess the effect of an uncertainty in the redshift distribution, we assume that the true distribution is given by Eq. (9) with $z_0=0.5$, while we “erroneously” assume the same form with $z_0=0.55$ [recall, $n(z)$ peaks at $z=2z_0$]. The biases in Ω_X and w are given in Table II, and are 1.2 and 3.0 times the unbiased 1σ uncertainties in these parameters, respectively. Just as in the case of the NLPS, we conclude that accurate knowledge of the redshift distribution of galaxies will be crucial if weak lensing is to achieve its full potential.

C. Power spectrum covariance

Yet another important issue that we ignored so far is covariance of the convergence power spectrum. The shear (or convergence) field is expected to be non-Gaussian due to nonlinear gravitational processes. Therefore, measurements of P_l^κ are generally going to be correlated, implying a non-zero four-point function (or its Fourier analogue, the trispectrum). The covariance will be especially pronounced at high multipoles. For a survey down to a limiting magnitude of $R\sim 25$, the effect of power spectrum covariance appears to be small: Cooray and Hu [67] have used the dark-matter halo approach to compute the power spectrum as well as the trispectrum, and found that the non-Gaussianity increases errors on cosmological parameters by about 15%. Although this effect is small enough to be ignored with current datasets, it will be important to take it into account when interpreting results from upcoming deep surveys because the covariance on small scales is likely to significantly degrade the cosmological constraints. Restricting our analysis (with COBE+photo- z prior) to multipoles $l\leq 3000$ degrades the constraints on Ω_X and w by a factor of 5. Clearly, information from small scales is important, and it will be necessary to carefully assess the impact of power spectrum covariance for deep WL surveys.

VII. THREE-POINT STATISTICS AND DARK ENERGY

We now turn to three-point statistics of the weak lensing convergence. Unlike the CMB temperature fluctuations which may or may not be Gaussian, weak lensing convergence almost certainly does not obey Gaussian statistics. In this section, we illustrate the dependence of the bispectrum and skewness of the convergence on dark energy, and show that they present a promising avenue that can lead to the dark component (see also Ref. [68]).

A. Preliminaries

The bispectrum of the convergence $B_{l_1 l_2 l_3}^\kappa$ is defined through the three-point correlation function of the convergence in multipole space

$$\langle \kappa_{l_1 m_1} \kappa_{l_2 m_2} \kappa_{l_3 m_3} \rangle = \begin{pmatrix} l_1 & l_2 & l_3 \\ m_1 & m_2 & m_3 \end{pmatrix} B_{l_1 l_2 l_3}^\kappa \quad (33)$$

and can further be written as

$$B_{l_1 l_2 l_3}^\kappa = \sqrt{\frac{(2l_1+1)(2l_2+1)(2l_3+1)}{4\pi}} \begin{pmatrix} l_1 & l_2 & l_3 \\ 0 & 0 & 0 \end{pmatrix} \times \left[\int d\chi \frac{[W(\chi)]^3}{r(\chi)^4} B\left(\frac{l_1}{r(\chi)}, \frac{l_2}{r(\chi)}, \frac{l_3}{r(\chi)}, \chi\right) \right]. \quad (34)$$

The bispectrum is defined only if the following relations are satisfied: $|l_j - l_k| \leq l_i \leq |l_j + l_k|$ for $\{i, j, k\} \in \{1, 2, 3\}$ and $l_1 + l_2 + l_3$ is even. The term in parentheses is the Wigner $3j$ symbol, which is closely related to Clebsch-Gordan coefficients from quantum mechanics (for its properties, see Refs. [69,70]). $W(\chi)$ is the weight function defined in Sec. II. To compute the bispectrum of the convergence, therefore, we need to supply the matter bispectrum $B(k_1, k_2, k_3, z)$. The latter quantity can be calculated in linear theory (that is, on large scales), but, just as in the case of the matter power spectrum, it needs to be calibrated from N -body simulations on nonlinear scales. Here we adopt the fitting formulas of Scoccimarro and Couchman ([71]; heretofore SC) which are based on numerical simulations due to VIRGO collaboration [72]. The matter bispectrum is defined only for closed-triangle configurations ($\vec{k}_1 + \vec{k}_2 + \vec{k}_3 = 0$) and is given by

$$B(\vec{k}_1, \vec{k}_2, \vec{k}_3) = 2 F_2(\vec{k}_1, \vec{k}_2) P(k_1) P(k_2) + \text{cycl.} \quad (35)$$

where $P(k)$ is the matter power spectrum and

$$F_2(\vec{k}_1, \vec{k}_2) = \frac{5}{7} a(n, k_1) a(n, k_2) + \frac{1}{2} \frac{\vec{k}_1 \cdot \vec{k}_2}{k_1 k_2} \left(\frac{k_1}{k_2} + \frac{k_2}{k_1} \right) \times b(n, k_1) b(n, k_2) + \frac{2}{7} \left(\frac{\vec{k}_1 \cdot \vec{k}_2}{k_1 k_2} \right)^2 c(n, k_1) c(n, k_2). \quad (36)$$

$n \equiv d \ln P / d \ln k$, and functions a, b and c are given in SC. Although not explicitly tested on models involving dark energy, the fitting formula depends on cosmology only through the matter power spectrum; this weak dependence on cosmology is also borne out in high-order perturbation theory [75]. Therefore, we decide to use the SC formula to illustrate the dependence of three-point statistics on dark energy.

In Fig. 11 we show the quantity $l^2 \sqrt{B_{lll}^\kappa} / (2\pi)$ [74] for $w = -1$ and $w = -0.5$; here B_{lll}^κ is the equilateral triangle configuration of the bispectrum.¹¹ Since roughly $B \propto P^2$ and B has little other dependence on dark energy, we expect that $l^2 \sqrt{B_{lll}^\kappa} / (2\pi)$ varies with w similarly as P — and this is correct (compare Figs. 2 and 11). Therefore, the bispectrum appears to be an excellent probe of dark energy. Things are complicated, however, by the large cosmic variance of a bispectrum. Although computing variance of B involves a daunting task of evaluating the six-point correlation function of the convergence, this quantity can be computed under an assumption of small departures from Gaussianity [76,77].

¹¹We set $m_\nu = 0$ in this section.

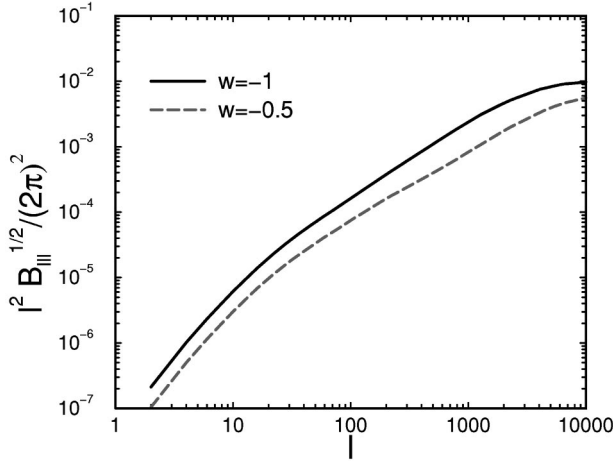


FIG. 11. The quantity $l^2 B_{III}^{1/2}/(2\pi)^2$, involving equilateral-triangle configurations of the bispectrum in multipole space. We use this quantity to illustrate how the bispectrum depends on dark energy. The variance in B_{III} is roughly two orders of magnitude larger than the signal.

For the equilateral triangle configuration of the bispectrum we show, this estimate indicates that the cosmic variance is about two orders of magnitude larger than the bispectrum signal itself, roughly independently of l . Therefore, it is unlikely that a single configuration of the bispectrum can be used to probe dark energy. However, one should be able to find an optimal combination of configurations in order to maximize the amount of information. We relegate this problem to future work.

Next we discuss the dependence of skewness on dark energy. Skewness is defined as

$$S_3(\theta) = \frac{\langle \kappa^3(\theta) \rangle}{\langle \kappa^2(\theta) \rangle^2} \quad (37)$$

where

$$\langle \kappa^2(\theta) \rangle = \frac{1}{4\pi} \sum_l (2l+1) P_l^\kappa \mathcal{W}_l^2(\theta) \quad (38)$$

$$\begin{aligned} \langle \kappa^3(\theta) \rangle &= \frac{1}{4\pi} \sum_{l_1 l_2 l_3} \sqrt{\frac{(2l_1+1)(2l_2+1)(2l_3+1)}{4\pi}} \\ &\quad \times \begin{pmatrix} l_1 & l_2 & l_3 \\ 0 & 0 & 0 \end{pmatrix} B_{l_1 l_2 l_3}^\kappa \mathcal{W}_{l_1}(\theta) \mathcal{W}_{l_2}(\theta) \mathcal{W}_{l_3}(\theta) \end{aligned} \quad (39)$$

are the second and third moments of the map smoothed over some angle θ , and $\mathcal{W}_l(\theta)$ is the Fourier transform of the top-hat function: $\mathcal{W}_l(\theta) = 2J_1(l\theta)/(l\theta)$. Skewness effectively combines many different bispectrum configurations, and its variance should be much smaller than that of $B_{l_1 l_2 l_3}$. Its disadvantage is that measurements on different scales are correlated.

Figure 12 shows skewness for two values of w . Roughly speaking, $S_3 \propto B^\kappa/P^2$, and although B^κ and P^2 both decrease

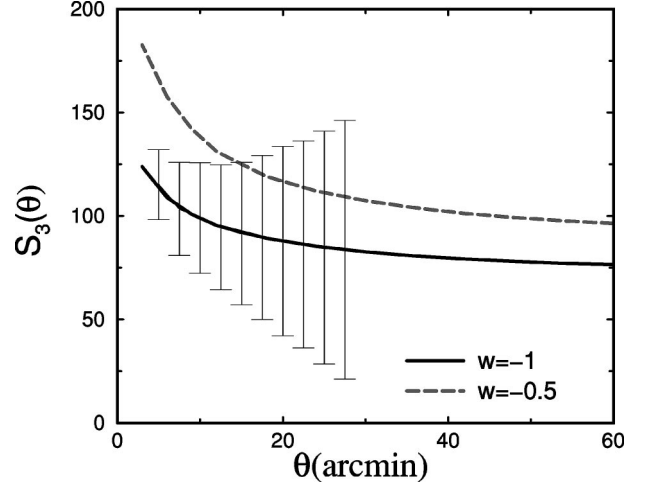


FIG. 12. Skewness of the convergence for two values of w . Error bars are from simulations by White and Hu [78] on scales they explore and for a field of 36 sq deg.

with increasing w , the P^2 term prevails — hence the scaling of S_3 with w . The error bars shown are those from White and Hu [78] for their WL simulations corresponding to the Λ CDM model, and for a field of 36 sq deg. Although the dependence of skewness on dark energy is significant, there are several obstacles. As in the case of the matter power spectrum, the fitting formula for the bispectrum is accurate only to about 15% (rms deviation) for Λ CDM models and not yet calibrated for dark energy models. More seriously, the measurements of skewness are likely to be highly correlated — in fact, van Waerbeke *et al.* [73] find that correlation between skewness measurements (for the top-hat filter we use) is close to 100%.

In conclusion, our preliminary analysis indicates that the three-point statistics of the weak lensing convergence are sensitive to the presence of dark energy, mainly through the dependence of the matter power spectrum. More work is needed, however, in order for the three-point statistic to become an effective probe of the missing component. This will include sharpening the predictions for the three-point function in the nonlinear regime, and finding optimal configurations of the bispectrum to probe dark energy.

VIII. DISCUSSION AND CONCLUSIONS

Recent results coming from type Ia supernovae, CMB, and large-scale structure surveys make a strong case for the existence of dark energy. It is therefore important to explore how upcoming and future surveys can be used to probe this component. In this work, we explore the power of weak gravitational lensing to probe dark energy via its measurements of the power spectrum of the convergence.

Dark energy modifies the convergence power spectrum by altering the distance-redshift relation, as well as the matter power spectrum. The dependence on dark energy is therefore somewhat indirect, and cannot be easily disentangled from the effect of other parameters ($\Omega_M h^2, \Omega_B h^2, n, m_\nu$). Because of this, one would not expect WL to be an efficient way to probe dark energy. Nevertheless, we find that with the pro-

posed very wide and deep surveys, WL can be an important probe of dark energy, on a par with SNe Ia and number counts. We consider a generic future survey covering 1000 sq deg down to a limited magnitude of $R=27$, cosmic-variance limited on large scales and Poisson-noise limited on small scales. With photometric redshift information and constraints on other parameters that would be expected from the Planck experiment with temperature information only, we find that such a survey is able to constrain Ω_X and w to between a few percent and a few tens of percent, depending on the fiducial model and a chosen set of priors. The constraints are in general stronger for wider and deeper surveys, and depend on the fiducial model (e.g., the neutrino mass). Accurate knowledge of the redshift distribution of source galaxies will be crucial; we find that an error of only 0.05 in the peak of the redshift distribution can bias the results.

There are important caveats to this result, however. Most information from WL comes from nonlinear scales, where the evolution of density perturbations is difficult to track analytically and understood mostly through N -body simulations (restricting the analysis of P_l^K only to linear scales with $l \leq 100$ would lead to extremely weak constraints on cosmological parameters due to cosmic variance). The nonlinearities potentially lead to at least two sources of systematic error. First, the power spectrum measurements P_l^K are likely to be strongly correlated at multipoles of several thousand and higher. This is especially true for planned deep surveys (down to a limited magnitude of $R \sim 27$ or higher), and these correlations will likely degrade the constraints on Ω_X and w .

Second, although the nonlinear power spectrum has been calibrated quite accurately for Λ CDM models, most notably through the PD formula, it remains poorly explored for models with general equation of state w , massive neutrinos, and significant baryon density. We explicitly showed that the lack of knowledge of the dependence of the nonlinear power spectrum on w can easily bias the constraints on Ω_X and w . Therefore, a better understanding and calibration of the NLPS is absolutely crucial in order to use WL as a tool of precision cosmology.

This problem can be turned around, however. One could use the weak lensing measurements (combined, perhaps, with information from CMB measurements, SNe Ia, and other probes) in order to *constrain* the nonlinear power spectrum. This constraint could be very interesting, given the

strong dependence of the NLPS on cosmological parameters.

Predictions for the three-point statistics of WL are quite uncertain at present, especially for models involving dark energy. This does not mean they will not become effective probes of the missing component in the future. We estimate the equilateral bispectrum configuration, as well as skewness, for two values of w and show that dependence on w is significant. Although these two quantities are plagued by large cosmic variance and highly correlated noise respectively, by clever choice of bispectrum configurations one might be able to increase the signal-to-noise ratio and extract useful information on dark energy.

There are other ways to use weak lensing as a probe of cosmology which we did not discuss. For example, one could use WL to identify clusters of galaxies at redshifts $0 < z \leq 3$ [M. Joffre *et al.* (in preparation)]. Comparing the measured number density of clusters to the prediction given by the formalism of Press and Schechter [79] gives constraints on cosmology. Another idea is to measure the angular power spectrum of clusters (detected through WL) at different redshifts [80]; this gives a direct measure of the angular diameter distance as a function of redshift. The advantage of this approach is that only the *linear* matter power spectrum is required; furthermore, the mass function and profiles of clusters need not be known. These two methods will provide constraints complementary to those from the galaxy shear.

Weak gravitational lensing is likely to provide a wealth of information not only on the matter distribution in the universe, but also on the amount and nature of dark energy. We have considered the basic program of measuring the convergence power spectrum, and found that very wide and deep surveys could provide information complementary and comparable to that from other cosmological probes. Other statistics (various bispectrum configurations, cross-correlation of WL and the CMB, etc.) are likely to further increase the power of weak lensing and make it an important probe of dark energy.

ACKNOWLEDGMENTS

The author would like to thank Asantha Cooray, Vanja Dukić, Joshua Frieman, Gil Holder, Mike Joffre, Michael Turner, and especially Wayne Hu for many useful discussions.

-
- [1] A. Riess *et al.*, *Astron. J.* **116**, 1009 (1998).
 - [2] S. Perlmutter *et al.*, *Astrophys. J.* **517**, 565 (1999).
 - [3] D. Huterer and M.S. Turner, *Phys. Rev. D* **60**, 081301(R) (1999).
 - [4] J. Weller and A. Albrecht, Report No. DAMTP-2001-53, astro-ph/0106079.
 - [5] I. Maor, R. Brustein, and P.J. Steinhardt, *Phys. Rev. Lett.* **86**, 6 (2001).
 - [6] M. Goliath, R. Amanullah, P. Astier, A. Goobar, and R. Pain, astro-ph/0104009.
 - [7] M.S. Turner, *Phys. Scri.*, T **T85**, 210 (2000).
 - [8] D. Huterer and M.S. Turner, *Phys. Rev. D* **64**, 123527 (2001).
 - [9] Z. Haiman, J.J. Mohr, and G.P. Holder, *Astrophys. J.* **553**, 545 (2001).
 - [10] J. Newman and M. Davis, *Astrophys. J. Lett.* **534**, L11 (2000).
 - [11] J.A. Tyson, F. Valdes, J.F. Jarvis, and A.P. Mills Jr., *Astrophys. J. Lett.* **281**, L59 (1984).
 - [12] J. Miralda Escudé, *Astrophys. J.* **380**, 1 (1991).
 - [13] R. Blanford, A. Saust, T. Brainerd, and J. Villumsen, *Mon. Not. R. Astron. Soc.* **251**, 600 (1991).
 - [14] N. Kaiser, *Astrophys. J.* **388**, 272 (1992).
 - [15] N. Kaiser, *Astrophys. J.* **498**, 26 (1998).
 - [16] B. Jain and U. Seljak, *Astrophys. J.* **484**, 560 (1997).

- [17] M. Kamionkowski, A. Babul, C.M. Cress, and A. Refregier, *Mon. Not. R. Astron. Soc.* **301**, 1064 (1998).
- [18] N. Kaiser and G. Squires, *Astrophys. J.* **404**, 441 (1993).
- [19] Y. Mellier, in *Proceedings of the NATO Advanced Study Institute on Theoretical and Observational Cosmology*, edited by Marc Lachieze-Rey (Kluwer Academic, Dordrecht, 1999), astro-ph/9901116.
- [20] D. Wittman, J.A. Tyson, D. Kirkman, I. Dell'Antonio, and G. Bernstein, *Nature (London)* **405**, 143 (2000).
- [21] D.J. Bacon, A.R. Refregier, and R.S. Ellis, *Mon. Not. R. Astron. Soc.* **318**, 625 (2000).
- [22] L. Van Waerbeke *et al.*, *Astron. Astrophys.* **358**, 30 (2000).
- [23] N. Kaiser, G. Wilson, and G.A. Luppino, astro-ph/0003338.
- [24] M.S. Turner and M. White, *Phys. Rev. D* **56**, R4439 (1997).
- [25] F. Bernardeau, L. Van Waerbeke, and Y. Mellier, *Astron. Astrophys.* **322**, 1 (1997).
- [26] W. Hu and M. Tegmark, *Astrophys. J. Lett.* **514**, L65 (1999).
- [27] C.B. Netterfield *et al.*, astro-ph/0104460.
- [28] C. Pryke *et al.*, astro-ph/0104490.
- [29] R. Stompor *et al.*, *Astrophys. J. Lett.* **561**, L7 (2001).
- [30] X. Wang, M. Tegmark, and M. Zaldarriaga, astro-ph/0105091.
- [31] M. Bartelmann and P. Schneider, *Phys. Rep.* **340**, 291 (2001).
- [32] W. Hu and M. White, *Astrophys. J. Lett.* **519**, L9 (2000).
- [33] T. Broadhurst, astro-ph/9505010.
- [34] C.L. Bennett *et al.*, *Astrophys. J. Lett.* **464**, L1 (1996).
- [35] C.-P. Ma, R.R. Caldwell, P. Bode, and L. Wang, *Astrophys. J. Lett.* **521**, L1 (1999) (Ma QCDM).
- [36] E.F. Bunn and M. White, *Astrophys. J.* **480**, 6 (1997).
- [37] A. Liddle and D. Lyth, *Cosmological Inflation and Large-Scale Structure* (Cambridge University Press, Cambridge, England, 2000).
- [38] W. Hu and D.J. Eisenstein, *Astrophys. J.* **498**, 497 (1998).
- [39] S.M. Carroll, W.H. Press, and E.L. Turner, *Annu. Rev. Astron. Astrophys.* **30**, 499 (1992).
- [40] P.J.E. Peebles, *Principles of Physical Cosmology* (Princeton University Press, Princeton, NJ, 1993).
- [41] A.J.S. Hamilton, A. Matthews, P. Kumar, and E. Lu, *Astrophys. J. Lett.* **374**, L1 (1991).
- [42] J.A. Peacock and S.J. Dodds, *Mon. Not. R. Astron. Soc.* **267**, 1020 (1994) (PD).
- [43] C.-P. Ma, *Astrophys. J. Lett.* **508**, L5 (1998) (Ma LCDM).
- [44] M. Tegmark, A.N. Taylor, and A.F. Heavens, *Astrophys. J.* **480**, 22 (1997).
- [45] M. Zaldarriaga and U. Seljak, *Phys. Rev. D* **55**, 1830 (1997).
- [46] D. Eisenstein, W. Hu, and M. Tegmark, *Astrophys. J.* **518**, 2 (1999).
- [47] M. Tegmark, D.J. Eisenstein, W. Hu, and R. Kron, astro-ph/9805117.
- [48] G.P. Holder, Z. Haiman, and J.J. Mohr, *Astrophys. J. Lett.* (to be published); **560**, L111 (2001).
- [49] N. Metcalfe, T. Shanks, A. Campos, H.J. McCracken, and R. Fong, *Mon. Not. R. Astron. Soc.* **323**, 795 (2001).
- [50] D.W. Hogg *et al.*, *Astrophys. J.* **115**, 1418 (1998).
- [51] R. Croft, W. Hu, and R. Davé, *Phys. Rev. Lett.* **83**, 1092 (1999).
- [52] W. Hu, *Astrophys. J. Lett.* **522**, L21 (1999).
- [53] C. Wetterich, *Nucl. Phys.* **B302**, 668 (1988).
- [54] K. Coble, S. Dodelson, and J. Frieman, *Phys. Rev. D* **55**, 1851 (1997).
- [55] I. Zlatev, L. Wang, and P.J. Steinhardt, *Phys. Rev. Lett.* **82**, 896 (1999).
- [56] W. Hu, *Phys. Rev. D* **65**, 023003 (2002).
- [57] W. Hu, *Phys. Rev. D* **62**, 043007 (2000).
- [58] A. Kinkhabwala and M. Kamionkowski, *Phys. Rev. Lett.* **82**, 4172 (1999).
- [59] H.V. Peiris and D.N. Spergel, *Astrophys. J.* **540**, 605 (2000).
- [60] D.J. Bacon, A. Refregier, D. Clowe, and R.S. Ellis, *Mon. Not. R. Astron. Soc.* **325**, 1065 (2001).
- [61] R.G. Crittenden, P. Natarajan, U.-L. Pen, and T. Theuns, *Astrophys. J.* **559**, 552 (2001).
- [62] R. Croft and C. Metzler, *Astrophys. J.* **545**, 561 (2000).
- [63] A. Heavens, A. Refregier, and C. Heymans, *Mon. Not. R. Astron. Soc.* **319**, 649 (2000).
- [64] U.-L. Pen, J. Lee, and U. Seljak, *Astrophys. J. Lett.* **543**, L107 (2000).
- [65] M.L. Brown, A.N. Taylor, N.C. Hambly, and S. Dye, astro-ph/0009499.
- [66] L. Knox, R. Scoccimarro, and S. Dodelson, *Phys. Rev. Lett.* **81**, 2004 (1998).
- [67] A. Cooray and W. Hu, *Astrophys. J.* **554**, 56 (2001).
- [68] L. Hui, *Astrophys. J. Lett.* **519**, L9 (1999).
- [69] D.A. Varshalovich, A.N. Moskalev, and V.K. Khersonskii, *Quantum Theory of Angular Momentum* (World Scientific, Singapore, 1998).
- [70] A. Cooray and W. Hu, *Astrophys. J.* **534**, 533 (2000).
- [71] R. Scoccimarro and H. Couchman, *Mon. Not. R. Astron. Soc.* **325**, 1312 (2001).
- [72] A.R. Jenkins *et al.*, *Astrophys. J.* **503**, 37 (1998).
- [73] L. Van Waerbeke, T. Hamana, R. Scoccimarro, S. Colombi, and F. Berardeau, *Mon. Not. R. Astron. Soc.* **322**, 918 (2001).
- [74] A. Cooray and W. Hu, *Astrophys. J.* **548**, 7 (2001).
- [75] R. Scoccimarro, S. Colombi, J.N. Fry, J.A. Frieman, E. Hivon, and A. Melott, *Astrophys. J.* **496**, 586 (1998).
- [76] X. Luo, *Astrophys. J. Lett.* **427**, L71 (1994).
- [77] A. Gangui and J. Martin, *Mon. Not. R. Astron. Soc.* **313**, 323 (2000).
- [78] M. White and W. Hu, *Astrophys. J.* **537**, 1 (2000).
- [79] W.H. Press and P.L. Schechter, *Astrophys. J.* **187**, 425 (1974).
- [80] A. Cooray, W. Hu, D. Huterer, and M. Joffre, *Astrophys. J. Lett.* **557**, L7 (2001).